IOP Conf. Series: Earth and Environmental Science **105** (2018) 012017 doi:10.1088/1755-1315/105/1/012017

Pyrolysis of activated carbon from coconut shell and its characteristic in the $LiFePO_4$/V/C composite for lithium ion battery cathode

N Sofyan[1,2], A D Rachmawati[1], A Zulfia[1,2] and A Subhan[3]
[1] Department of Metallurgical and Materials Engineering, Faculty of Engineering, Universitas Indonesia, Depok 16424, Indonesia
[2] Tropical renewable Energy Center, Faculty of Engineering, Universitas Indonesia, Depok 16424, Indonesia
[3] Research Center for Physics, Indonesian Institute of Science (LIPI), Puspiptek Serpong, Cisauk-Banten, Indonesia 15314

E-mail: nofrijon.sofyan@ui.ac.id

Abstract. Most of the time, coconut shells from the coconut farms have not been used but for charcoal purpose. In this work, the charcoal from the coconut shells was converted into an activated carbon and used it for the development of lithium ion battery. The development was begun by firstly synthesizing $LiFePO_4$ (LFP) through a hydrothermal route using stoichiometric amounts of precursors LiOH, $NH_4H_2PO_4$, and $FeSO_4.7H_2O$. The as-synthesized LFP was then mixed with variation of vanadium concentrations and a fix concentration of the carbon pyrolyzed from the coconut shells. X-ray diffraction (XRD) was used to characterize the crystal structure, whereas a scanning electron microscope (SEM) was used to characterize surface morphology of the composite. The characteristic of the composite was further examined an electrochemical impedance spectroscopy (EIS) for the conductivity. The XRD results showed that the $LiFePO_4$/V/C has been formed successfully with an olivine structure. The SEM results depicted an agglomerate morphology but most of $LiFePO_4$/V particles have been coated by the carbon. The EIS results showed conductivity values of $1.3387x10^{-2}$ S/cm, $1.184x10^{-3}$ S/cm, $1.7241x10^{-3}$ S/cm, and $6.6423x10^{-4}$ S/cm for the LFP/C-0V, LFP/C-3V, LFP/C-5V, and LFP/C-7V samples, respectively. The performance test indicated that coconut shell has a great potential as a cheap carbon resource for the development of lithium ion battery cathode.

1. Introduction

Indonesia is one of the largest coconut producers in the world with a plantation area of 2.526 million hectares and a total production of 2.833 million tons in 2016 [1]. In its processing, the commonly used coconut commodity is the inner white meat for copra and oil extraction, while the rest as a shell will be wasted. This coconut shell waste, both in industrial and household scales, is usually discarded, or very few use for its charcoal purposes. At the same time, disposal of this amount of coconut waste would be a problem if a proper waste management and treatment is not performed. On the other hand, this waste could be turned into high value and useful products in many applications. Utilization of the coconut shell wastes as a source of activated carbon, for example, is one of the solutions to minimize the

coconut waste, to increase the coconut shell waste value, and at the same time to overcome the aforementioned problems.

Activated carbon is a form of carbon processed to have small particle size but with high pore volume and thus will increase the available surface area used in many applications [2]. The use of coconut shell derived activated carbon as an active anode material to improve the performance of lithium ion battery has been attempted by many investigators [3]. This activated carbon attracts many attentions because of its abundance, cost effective and environment friendly in nature [4]. It has also been known that activated carbon synthesized from coconut shell is considered to have a better performance in comparison to those obtained from other sources because of its mesoporous structure, which will make it more suitable for electrode material [5–7].

Lithium ferro phosphate ($LiFePO_4$) has attracted many attentions since the reversibility of intercalation-deintercalation lithium ion in electrochemical process was observed [8], primarily as a promising candidate for lithium ion battery cathode. Many advantages of this material have been reviewed such as low production cost, environmental friendly and high capacity and stability cycle [9]. However, despite its many advantageous, $LiFePO_4$ also has a drawback in its pure form due to its low electronic conductivity, measured only 10^{-9} S/cm [10]. This low electronic conductivity will result in a low rate capability. Because of that, many efforts have been proposed by many investigators to improve this conductivity, for example through a metal doping [11, 12], carbon coating [9], and co-synthesis with carbon in powder metallurgy method [13].

In this current work, $LiFePO_4$ was synthesized via sol-gel method followed by hydrothermal route. The electrochemical properties of the material were improved by using vanadium as a metal dopant along with the addition of activated carbon pyrolyzed from low cost coconut shell to form a composite of $LiFe_{1-x}V_xPO4/C$. The effects of carbon and vanadium on the structure, morphology and electrochemical performance of the composite used as cathode active material in lithium ion battery are reported and discussed in detail.

2. Experimental Setup

The raw material of coconut was collected from local market in Jakarta. After the white meat was removed from the hard shell and the thin brown rind was pared off, the coconut shell was thoroughly washed with tap water to remove any adhering dirt and dried under room temperature condition. The dried coconut shell was then pyrolyzed at 700 °C and the result in the form of coconut shell charcoal was crushed and sieved into fine carbon fragments. The steps in obtaining the coconut shell charcoal are given schematically in figure 1.

Figure 1. Steps in carbon pyrolysis from coconut shell. Left to right is coconut, coconut shells, chopped and dried coconut shells, and coconut shells after pyrolysis.

The as-prepared coconut fine carbon was then activated by soaking it in the H_3PO_4 0.75 M solution for 7 hours. After the soaking, the mixture was filtered using filter paper and the carbon precipitate was dried in an oven at 105 °C for 10 hours. The dried carbon was further washed with hot distilled water to obtain a pH 7 and was dried again in an oven at 100 °C for 12 hours. The activated carbon

was cooled to room temperature and ready for characterization using X-ray diffraction (XRD, ARL OPTX-2050) with Cu Kα radiation (λ = 1.5406 Å).

Lithium ferro phosphate, $LiFePO_4$, was synthesized in according to our previous work [14] and is explained as following. In a separated glass beaker, a stoichiometric amount of the precursors LiOH, $NH_4H_2PO_4$, and $FeSO_4.7H_2O$ (all analytical grade reagents from E-Merck) was dissolved in 30 ml distilled water. After dissolution, the three solutions were mixed into another glass beaker and was stirred until homogenized using a magnetic stirrer for 30 minutes. The homogenous mixed solution was then transferred into a Teflon autoclave and hydrothermally heated at 180ºC for 20 hours. The precipitates were separated from the solution and washed with deionized water several times before being dried in an oven at 80ºC for 18 hours. Crystal characteristics of the powder were examined using X-ray diffraction (XRD, ARL OPTX-2050) with Cu Kα (λ = 1.5406 Å).

The composites $LiFe_{1-x}V_xPO_4/C$ was prepared by firstly preparing the as-synthesized $LiFePO_4$ powders from the previous step each with variations of 0, 3, 5, and 7 wt.% H_4NO_3V in a ball mill. An amount of 3 wt.% activated carbon was then added into the mixture and the ball-milling process continued until a homogenized mixture was obtained. The mixture was then sintered at 750ºC for four hours under an argon environment. The characteristics of the resulting cathode active materials were examined by using X-ray diffraction (XRD, Philips PW3020) with Cu Kα radiation (λ = 1.5406 Å) and a scanning electron microscope (SEM, FEI Quanta-650) to characterize the morphology of the formed composites.

The cathode was prepared using the best active material in terms of crystal structure and homogeneity of the composites from the previous step. The selected material was mixed with poly-vinylidene fluoride (PVDF, MTI) in N-methyl pyrrolidone (NMP, MTI) solvent inside a vacuum mixer. The mixture in the form of paste was then applied onto a current collector of aluminium foil (MTI), dried, hot-rolled and heated in a vacuum oven at 80°C. The conductivity was further measured using an electrochemical impedance spectroscopy (EIS, Hioki LCR 3532-50).

3. Results and Discussion

X-ray diffraction was carried out to confirm the crystal structure of the sample by performing the test using Cu Kα radiation (λ = 1.5406 Å). The diffraction pattern is shown in figure 2. As seen in the figure, inset is the activated carbon from the coconut shell, (a) reference $LiFePO_4$, (b) commercial $LiFePO_4$, (c) as-synthesized $LiFePO_4$ with carbon addition only, (d) 0 wt.% V-doped $LiFePO_4/C$, (e) 3 wt.% V-doped $LiFePO_4/C$, (f) 5 wt.% V-doped $LiFePO_4/C$, and (g) 7 wt.% V-doped $LiFePO_4/C$. For the activated carbon from the coconut shell, as can be seen in the inset, the pyrolyzed sample shows the same diffraction patterns to that of the reference (Nixon et al, 1966) with a structure indexed to the rhombohedral R m space group (JCPDS 74-2328) but with the broaden peaks as an indication of amorphous tendency. The diffractograms show two peaks at around 25° and 43° corresponding to the crystalline reflections from (002) and (101) planes. No typical diffraction peaks of other phases are found in the diffraction patterns.

For the $LiFePO_4$ samples, all of the diffraction peaks of the as-synthesized samples with carbon addition are still in agreement with that of $LiFePO_4$ reference with a structure crystal indexed to the Pnma orthorhombic (JCPDS No.083-2092). This result is in agreement with the result found by others [15, 16]. The same result is true for the synthesized $LiFePO_4$ with carbon addition and various concentrations of up to 7 wt.% vanadium. Some discrepancies exist, however, in terms of impurities and or peaks shifting due to the carbon and or vanadium addition. This is specifically true for the as-synthesized $LiFePO_4$ and the $LiFePO_4$ with carbon addition only. As can be seen in figure 2(c) and (d), some other diffraction peaks are found in the diffractograms. These impurities that are yet to be confirmed could be due to the oxidation process occurred during the sintering process. The impurities peaks, however, are disappeared after vanadium addition at which no typical diffraction peaks of other phases are found in the diffraction patterns.

High crystallinity has been obtained in all of vanadium-doped $LiFePO_4/C$ indicated by strong and sharp diffraction peaks with no typical diffraction patterns of carbon nor vanadium as can be seen in

figure 2(e), 2(f), and 2(g). The non-existence of carbon and vanadium diffraction patterns within the materials is an indication that carbon could exists in an amorphous form and that vanadium has substituted and occupied Fe sites in $LiFePO_4$. It could be also that they have been dissolved into $LiFePO_4$ structure to form a solid solution of $LiFe_{1-x}V_xPO_4/C$ composite as expected.

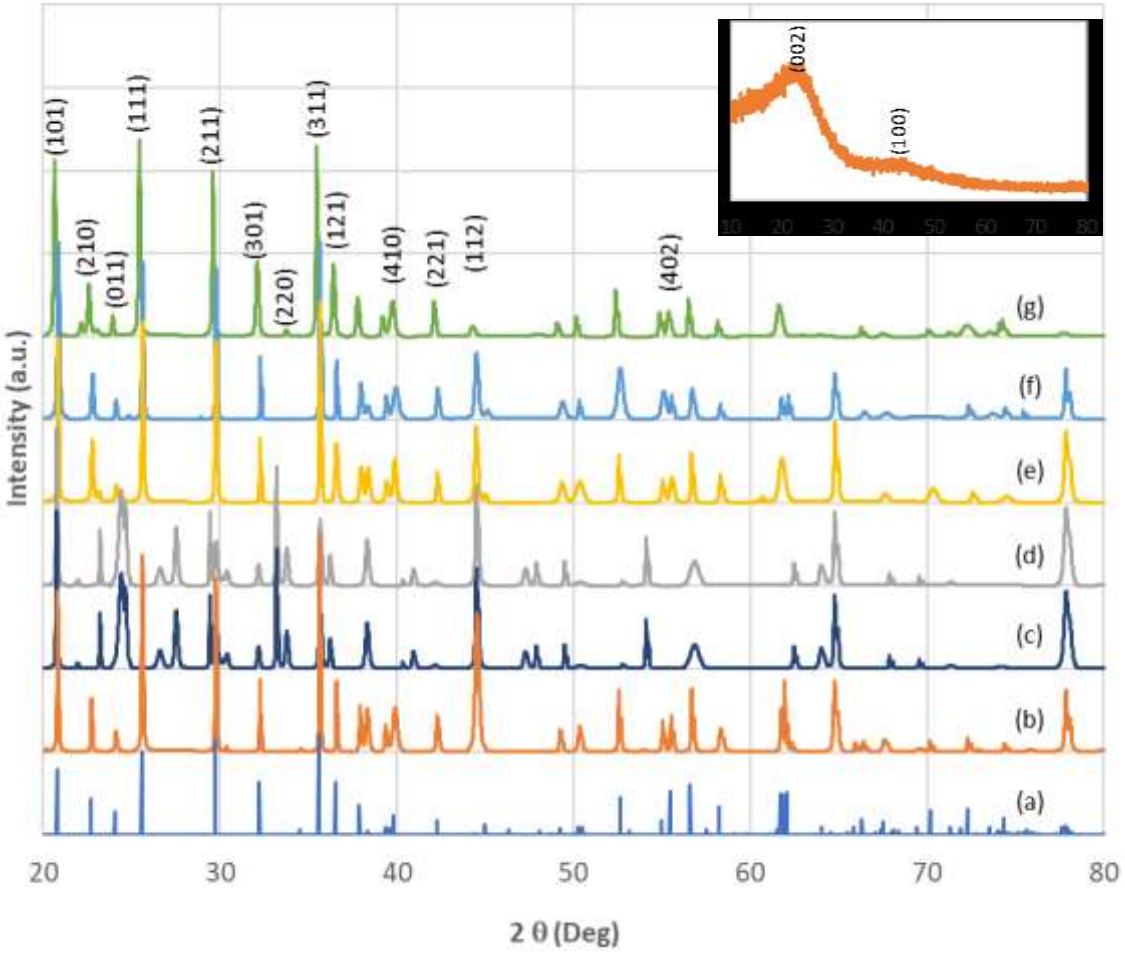

Figure 2. Diffraction patterns of (a) reference $LiFePO_4$, (b) commercial $LiFePO_4$, (c) as-synthesized $LiFePO_4$, (d) $LiFePO_4$/C at 0 wt.% V, (e) $LiFePO_4$/C at 3 wt.% V, (f) $LiFePO_4$/C at 5 wt.% V, and (f) $LiFePO_4$/C at 5 wt.% V. Inset is the X-ray diffraction pattern of the activated carbon from the coconut shell

Surface morphology of the as-synthesized activated carbon from the coconut shell, $LiFePO_4$, and the $LiFePO_4$/V/C composites was revealed using an electron microscope. The results from the secondary electron image are given in figure 3. Figure (a) is the activated carbon from the coconut shell, figure 3(b) is the as-synthesized $LiFePO_4$, figure (c) 0 wt.% V-doped $LiFePO_4$/C; (d) 3 wt.% V-doped $LiFePO_4$/C; (e) 5 wt.% V-doped $LiFePO_4$/C; (f) 7 wt.% V-doped $LiFePO_4$/C. There is a difference observed on the surface morphology of the composite between the as-synthesized $LiFePO_4$ and the one with the addition of activated carbon from the coconut shell. In figure 3(a), most of the particles in the as-synthesized activated carbon show the morphology of particles having flake shape and are still agglomerated. The same is true for the as-synthesized $LiFePO_4$, which is the characteristic of $LiFePO_4$ formed through a hydrothermal process [17] as can be seen in figure 3(b). However, the agglomeration tendency is reduced with the addition of carbon. Figure 3(c) shows the morphology of with no activated carbon. The sample has a round shape with a smaller particle than that of the as-

synthesized $LiFePO_4$. figure 3(d) is the morphology of $LiFePO_4$/C at 3 wt.% vanadium, figure 3(e) shows the morphology of $LiFePO_4$/C at 5 wt.% vanadium, and figure 3(f) shows the morphology of $LiFePO_4$/C at 7 wt.% vanadium. The morphology reveals that $LiFePO_4$/C agglomeration tendency is well reduced with the addition of vanadium and thus the particle distributes homogeneously at 7 wt.% vanadium.

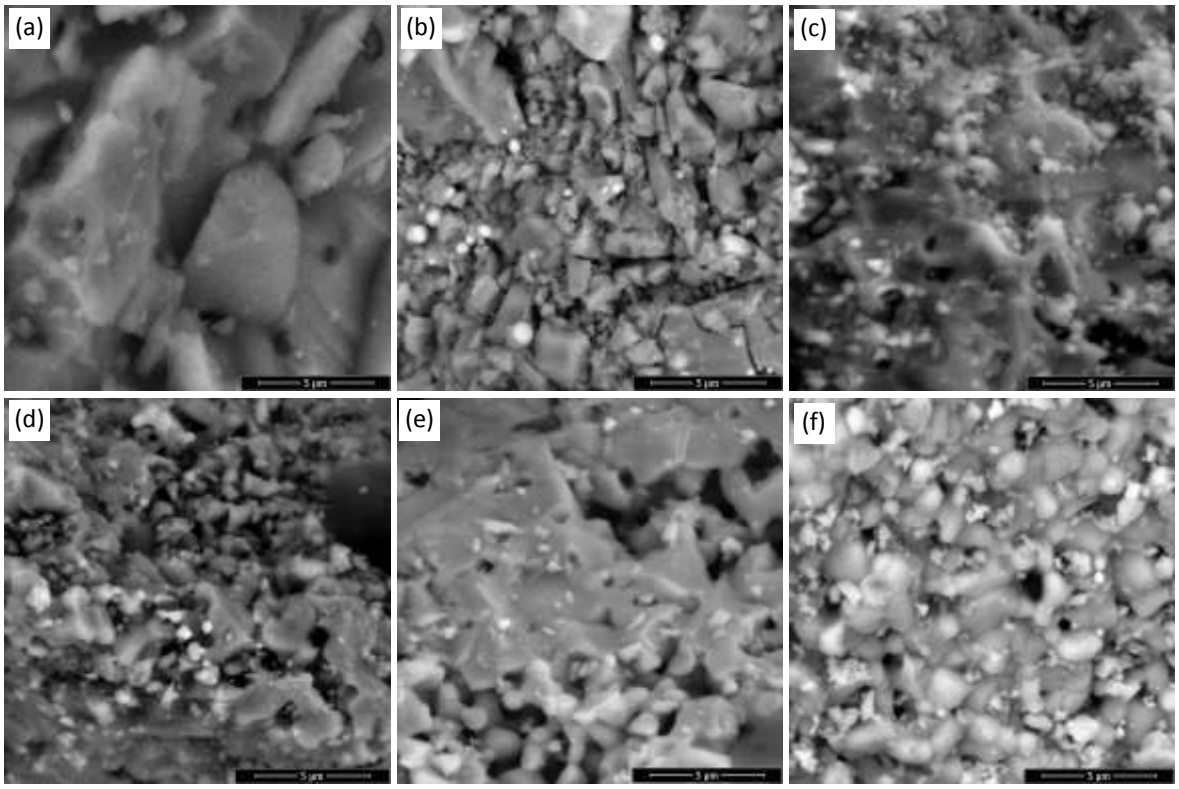

Figure 3. Secondary electron images of (a) activated carbon from the coconut shell; (b) as-synthesized $LiFePO_4$; (c) 0 wt.% V-doped $LiFePO_4$/C; (d) 3 wt.% V-doped $LiFePO_4$/C; (e) 5 wt.% V-doped $LiFePO_4$/C; and (f) 7 wt.% V-doped $LiFePO_4$/C. The bar scale is 5 μm.

Electrical conductivity was performed on the prepared composite cathode sheets using electrical impedance spectroscopy to show the conductivity through a plot diagram depicting the material's capacitance. The results in the forms of Cole plots are shown in figure 4.

As seen in figure 4, the testing was performed on a fix carbon composition and various vanadium concentrations to form $LiFePO_4$/C/V at 0 wt.% V, 3 wt.% V, 5 wt.% V and 7 wt.% V. Analysis of the Cole-Cole diagrams in figure 4 shows values of 1.3387×10^{-2} S/cm, 1.184×10^{-3} S/cm, 1.7241×10^{-3} S/cm, and 6.6423×10^{-4} S/cm for the LFP/C-0V, LFP/C-3V, LFP/C-5V, and LFP/C-7V samples, respectively. When compared to the pure $LiFePO_4$ [10], the carbon coated $LiFePO_4$ shows an increase of conductivity. This is due to the presence of high conductivity carbon that helps intercalation and deintercalation of the Li ion. In this work, however, all V-doped $LiFePO_4$/C samples shows a lower conductivity compared to that of carbon coated $LiFePO_4$. The uneven presence of vanadium and carbon and the presence of pores can increase resistance by forming a bulk layer that blocks and decreases the electrical conductivity.

Cyclic voltammetry and charge/discharge testing were performed for the two active materials only, i.e. $LiFePO_4$/C at 3 wt.% V and 7 wt.% V. The resulting curves are given in figure 5. As seen in figure 5, cyclic voltammetry curves shown at the top have reduction-oxidation peaks at 3.59 and 3.20 volts for 3 wt.% V (left) and at 3.59 and 3.05 volts for 7 wt.% V (right), respectively. The charge/discharge

testing of the composite was performed at the potential range of 2.5–4.2 V at two capacities, i.e. 0.5C and 4C, and the curves are shown at the bottom in figure 5 for the LiFePO4/C at 3 wt.% V (left) and 7 wt.% V (right). The initial charge and discharge capacities at 0.5C for LiFePO4/C at 7 wt.% V (4.8 mAh g^{-1}) are higher than that of 5 wt.% V (3.2 mAh g^{-1}), however, the charge and discharge capacity of 7 wt.% V drops below 1.2 mAh g^{-1} at 4C whereas for LiFePO4/C at 7 wt.% V, the capacity is still 1.6 mAh g^{-1}. It seems that, as has been mentioned previously, when the vanadium concentration is high, at low cycle, it can accommodate the high capacity. However, at higher cycle, the uneven presence of vanadium and carbon and the presence of pores starts forming a bulk layer that blocks and decreases the electrical conductivity and thus the capacity.

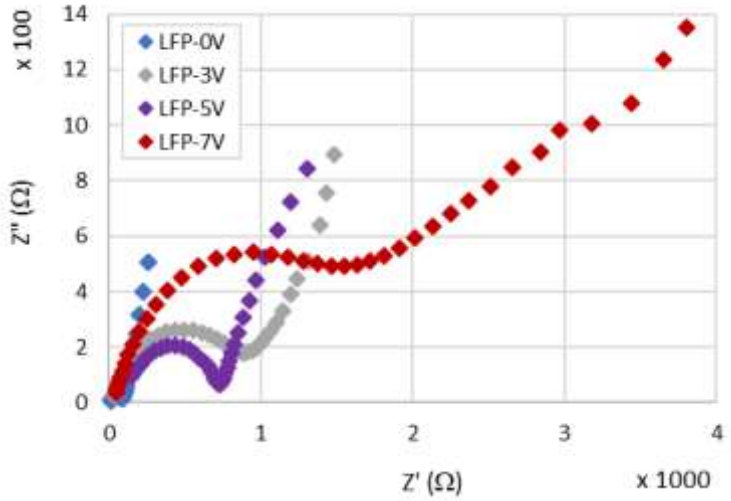

Figure 4. Cole-Cole plots of EIS test results for 0 wt.% V-doped, 3 wt.% V-doped, 5 wt.% V-doped, and 7wt.% V-doped $LiFePO_4$/C

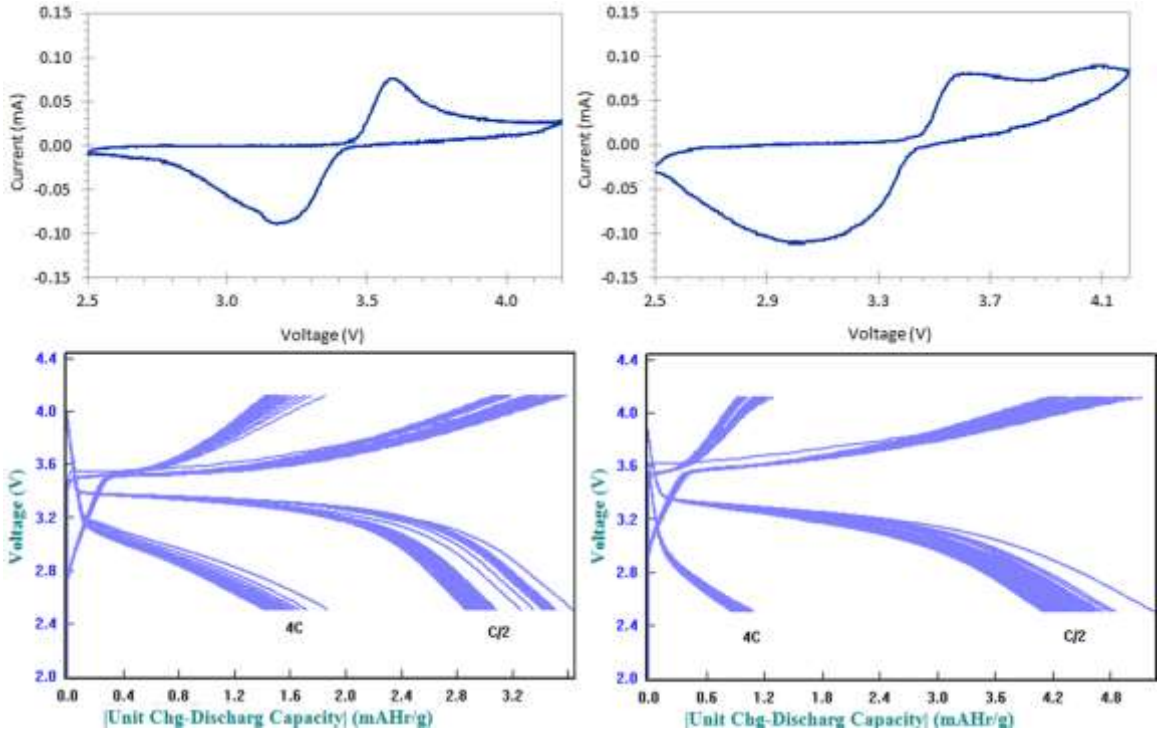

Figure 5. Cyclic voltammetry (top) and charge/discharge (bottom) curves for the $LiFePO_4$/V/C at 3 wt.% V (left) and 7 wt.% V (right)

4. Conclusion

In this work, the hydrothermal process has resulted in high purity of $LiFePO_4$ and morphologically formed agglomerated small particles containing $LiFePO_4$. The addition of activated carbon from the coconut shell did not affect the purity of the $LiFePO_4$ particles, however, the addition of vanadium shifts the triphylite peaks due to the emergence of the impurity phase. The addition of vanadium also decreases the conductivity because of uneven distribution of vanadium and carbon with a value of 1.3387×10^{-2} S/cm, 1.184×10^{-3} S/cm, 1.7241×10^{-3} S/cm, and 6.6423×10^{-4} S/cm for the LFP/C-0V, LFP/C-3V, LFP/C-5V, and LFP/C-7V samples, respectively.

5. Acknowledgement

The authors would like to express their gratitude and appreciation for the funding from the Directorate of Research and Community Services (DRPM), Universitas Indonesia, through Hibah PITTA No. 822/UN2.R3.1/HKP.05.00/2017.

6. References

[1] Subiyantoro M E and Arianto Y (Eds) 2016 *Tree Crop Estate Statistics of Indonesia 2014-2016* (Jakarta: Directorate General of Estate Crops)
[2] Ahmadpour A, Okhovat A, Mahboub M J D 2013 *J. Phys. Chem. Solids* **74** 886
[3] Hwang Y J, Jeong S K, Shin J S, Nahm K S, Stephan A M 2008 *J. Alloys Compd*. **448** 141
[4] Frackowiak E and Béguin F 2002 *Carbon* **40** 1775
[5] Zhou X, Li L, Dong S, Chen X, Han P, Xu H, Yao J, Shang C, Liu Z, and Cui G 2012 *J. Solid State Electrochem*. **16** 877
[6] Xiong W, Liu M, Gan L, Lv Y, Li Y, Yang L, Xu Z, Hao Z, Liu H and Chen L 2011 *J. Power Sources* **196** 10461
[7] Kuratani K, Okuno K, Iwaki T, Kato M, Takeichi N, Miyuki T, Awazu T, Majima M and Sakai T 2011 *J. Power Sources* **196** 10788
[8] Padhi A K, Nanjundaswamy K S and Goodenough J, 1997 *Electrochem. Soc* **144** 1188
[9] Hu L-H, Wu F Y, Lin C T, Khlobystov A N, and Li L J 2013 *Nature Commun* **4** 1687 1
[10] Chung S Y, Bloking J T and Chiang Y M 2002 *Nat. Mater*. **1** 123
[11] Arumugam D, Kalaignan G P and Manisankar P 2008 *J. Solid State Electrochem*. **13** 301
[12] Liu H, Xie J and Wang K 2008 *Solid State Ionics* **179** 1768
[13] Dominko R, Bele M, Gaberscek M, Remskar M, Hanzel D, Pejovnik S and Jamnik J 2005 *J. Electrochem. Soc*. **152** A607
[14] Sofyan N, Putro D Y and Zulfia A 2016 *Int. J. Technol*. **7** 1307
[15] Yang M R and Ke W H, 2008 *J. Electrochem. Soc*. **155** A729
[16] Teng T H, Yang M R, Wu S H 2007 *Solid State Commun*. **142** 389
[17] Shu H, Wang X, Wu Q, Liang Q, Yang X, Yang S, Liu L, Wei Q, Hu B, Zhou M, Chen M, and Zhang L 2012 *J. Electrochem. Soc*. **159** A1904